Supporting Information

Identification of the Structure of the Bi Promoted Pt Non-oxidative Coupling of Methane Catalyst: A Nanoscale Pt_3Bi Intermetallic Alloy

Johnny Zhu Chen,[1] Zhenwei Wu,[1,2] Xiaoben Zhang,[3] Slgi Choi,[1] Yang Xiao,[1] Arvind Varma,[1] Wei Liu,[3] Guanghui Zhang,[1,4]* and Jeffrey T. Miller[1]*

[1] Davidson School of Chemical Engineering, Purdue University, 480 Stadium Mall Drive, West Lafayette, IN 47907, United States
[2] School of Chemical Engineering, Stanford University, 381 North-South Mall, Stanford, CA 94305, United States.
[3] Dalian Institute of Chemical Physics, Chinese Academy of Sciences, Dalian, Liaoning 116023, China
[4] State Key Laboratory of Fine Chemicals, PSU-DUT Joint Center for Energy Research, School of Chemical Engineering, Dalian University of Technology, Dalian, Liaoning 116024, China

E-mails: gzhang@dlut.edu.cn, mill1194@purdue.edu

Mears Criterion for External Diffusion Limitations

External diffusion are negligible if $\frac{r_{obs} \cdot \rho_{cat} \cdot R \cdot n}{k_c \cdot C} < 0.15$

r_{obs}- measured reaction rate, mol/(g_{cat} · s)

ρ_{cat}- catalyst density, g/m^3

R- catalyst pellet radius, m

n- reaction order

k_c- mass transfer coefficient, m/s

C- bulk concentration

For propane dehydrogenation at 550°C for the most active catalyst 2Pt/SiO_2:

$r_{obs} = 1.77 \cdot 10^{-5}\ mol/(gcat \cdot s)$, $\rho_{cat} = 2.65 \cdot 10^6$ g/m^3, R = $4.20 \cdot 10^{-4}$ m, n=1, k_c= 0.214 m/s, C= 0.370 mol/m^3

$$\frac{r_{obs} \cdot \rho_{cat} \cdot R \cdot n}{k_c \cdot C} = 2.48 \cdot 10^{-3} < 0.15$$

Weisz-Prater criterion for Internal Diffusion Limitations

Internal diffusion are negligible if $\Psi = \frac{n+1}{2} \cdot \frac{r_{obs} \cdot \rho_{cat} \cdot R^2}{D \cdot C} < 1$

n- reaction order

r_{obs}- measured reaction rate, mol/(g_{cat} · s)

ρ_{cat}- catalyst density, g/m^3

R- catalyst pellet radius, m

D- diffusion coefficient, m^2/s

C- bulk concentration

For propane dehydrogenation at 550°C for the most active catalyst 2Pt/SiO_2:

n=1, $r_{obs} = 1.77 \cdot 10^{-5}\, mol/(gcat \cdot s)$, $\rho_{cat} = 2.65 \cdot 10^{6}$ g/m^3, $R = 4.20 \cdot 10^{-4}$ m, D=1 $\cdot 10^{-4}$ m, C= 0.370 mol/m^3

$$\Psi = \frac{n+1}{2} \cdot \frac{r_{obs} \cdot \rho_{cat} \cdot R^2}{D \cdot C} = 0.223 < 1$$

Mears Criterion for External Heat Transfer Limitations

External heat transfers are negligible if $\frac{r_{obs} \cdot \rho_{cat} \cdot R \cdot E_a \cdot \Delta H}{k_g \cdot R_g \cdot T^2} < 0.15$

r_{obs}- measured reaction rate, mol/(g_{cat} · s)

ρ_{cat}- catalyst density, g/m^3

R- catalyst pellet radius, m

E_a- activation energy, J/mol

ΔH- reaction heat, J/mol

k_g- heat transport coefficient, J/(m^2·s·K)

R_g – gas constant, J/(mol·K)

T – reaction temperature, K

For propane dehydrogenation at 550°C for the most active catalyst 2Pt/SiO_2:

$r_{obs} = 1.77 \cdot 10^{-5}\, mol/(gcat \cdot s)$, $\rho_{cat} = 2.65 \cdot 10^{6}$ g/m^3, $R = 4.20 \cdot 10^{-4}$ m, $E_a = 1.20 \cdot 10^{5}$ J/mol, ΔH= $1.29 \cdot 10^{5}$ J/mol, $k_g = 1.46 \cdot 10^{3}$ J/(m^2·s·K), R_g= 8.31 J/(mol·K),T=823 K

$$\frac{r_{obs} \cdot \rho_{cat} \cdot R \cdot E_a \cdot \Delta H}{k_g \cdot R_g \cdot T^2} = 3.71 \cdot 10^{-2} < 0.15$$

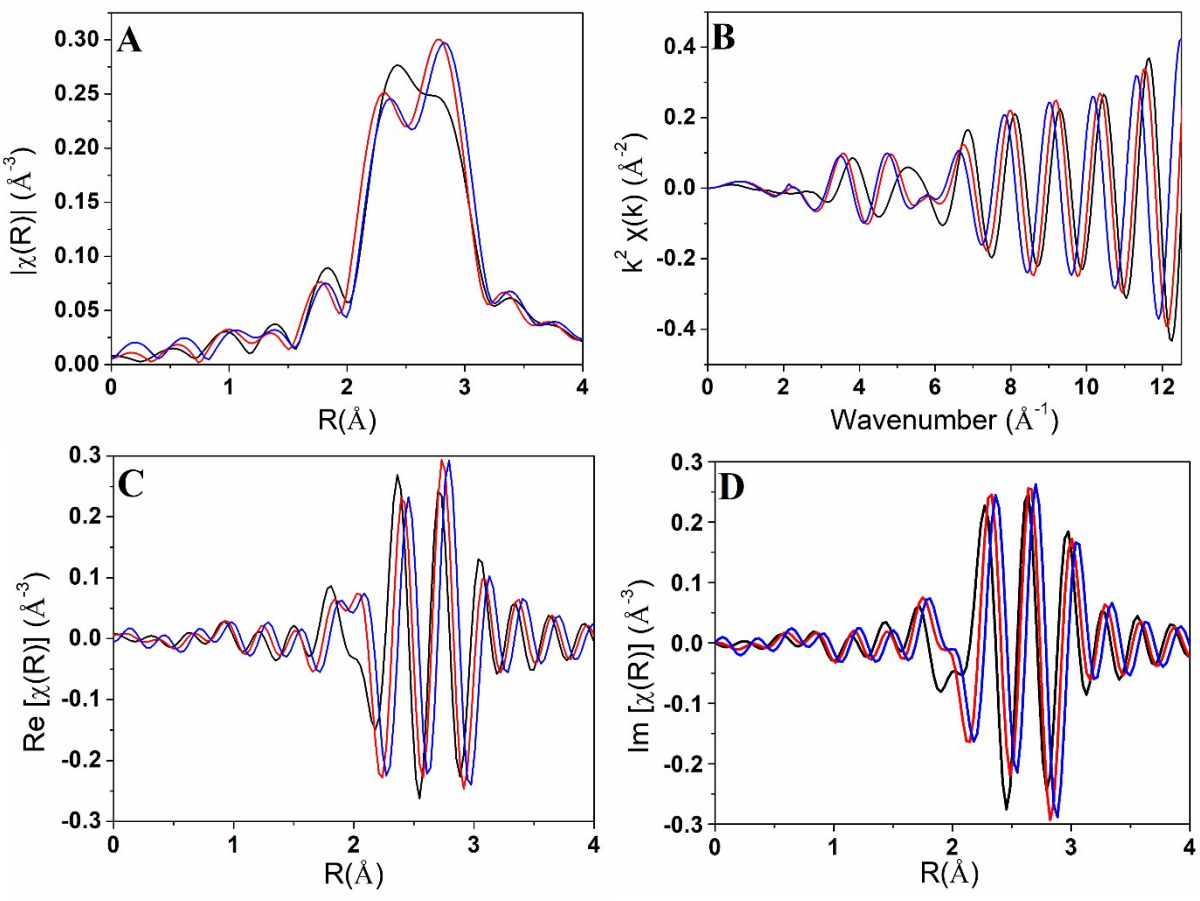

Figure S1. Pt L3 edge EXAFS spectra FEFF calculation: A) R space FT magnitude, B) k space, C) R space FT real part and D) R space FT imaginary part. Pt-Pt at R=2.75 Å (black), Pt-Bi at R=2.75 Å (red), Pt-Bi at R=2.80 Å (blue).

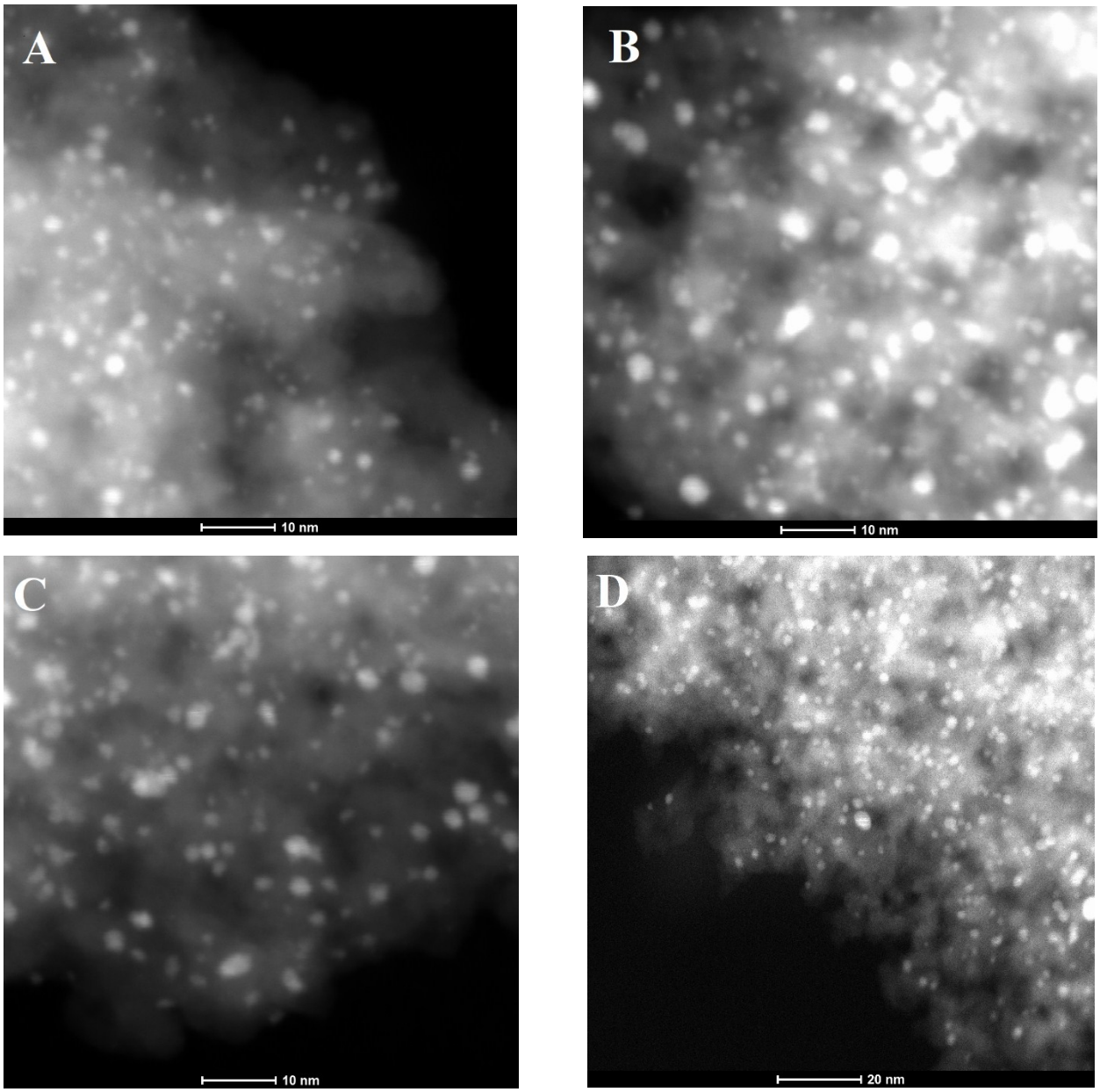

Figure S2. STEM HAADF images of A) 2Bi-2Pt/SiO_2 (2.7±0.5 nm), B) 4Bi-2Pt/SiO_2 (2.3±0.5 nm), C) 2Pt/SiO_2 (2.2±0.4 nm), D) 1Bi-2Pt/SiO_2 (2.7±0.4 nm)

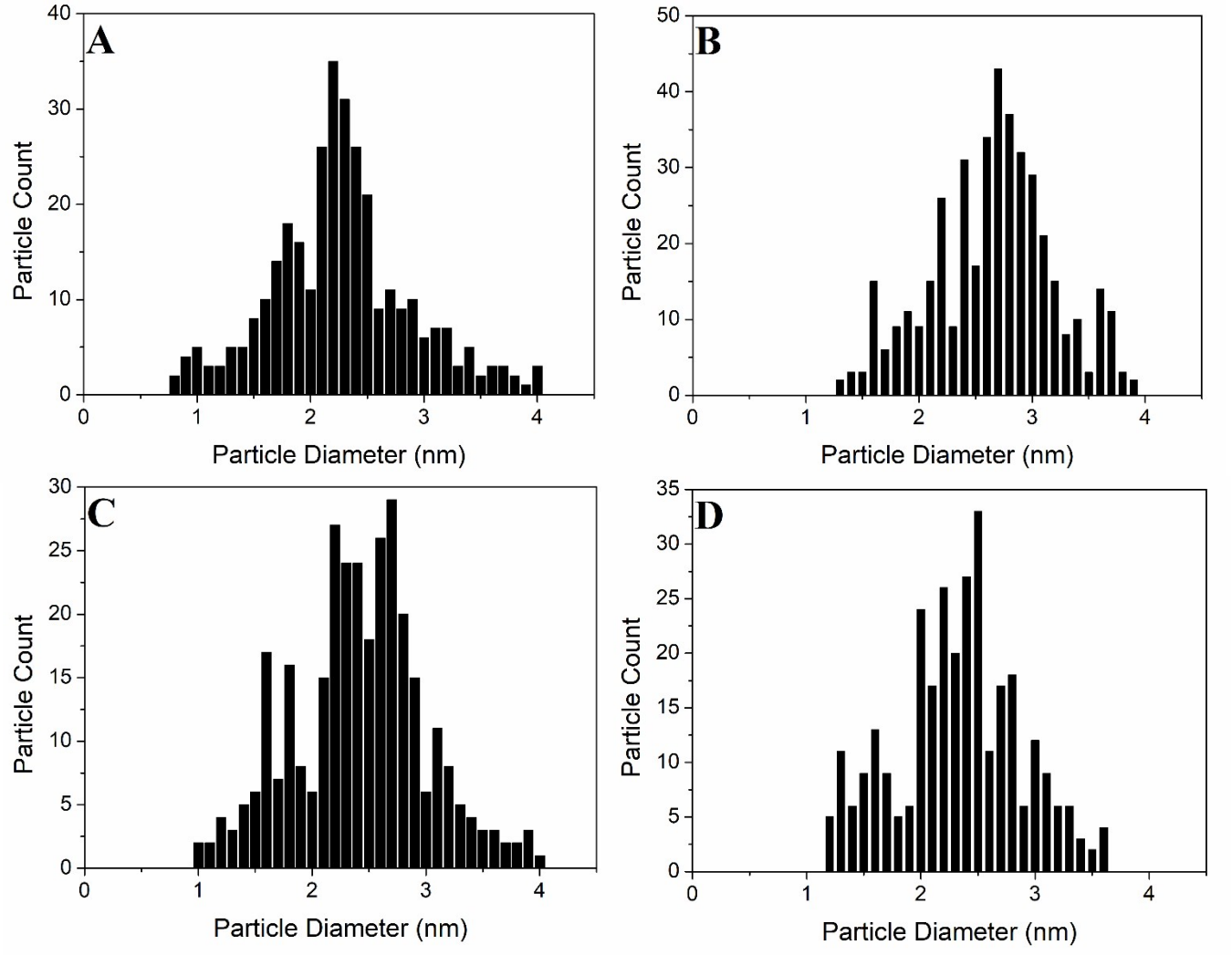

Figure S3. Particle size distribution statistics of A) 2Pt/SiO_2 (2.2±0.6 nm), B) 1Bi-2Pt/SiO_2 (2.7±0.5 nm) C) 2Bi-2Pt/SiO_2 (2.4±0.5 nm), D) 4Bi-2Pt/SiO_2 (2.3±0.5 nm)

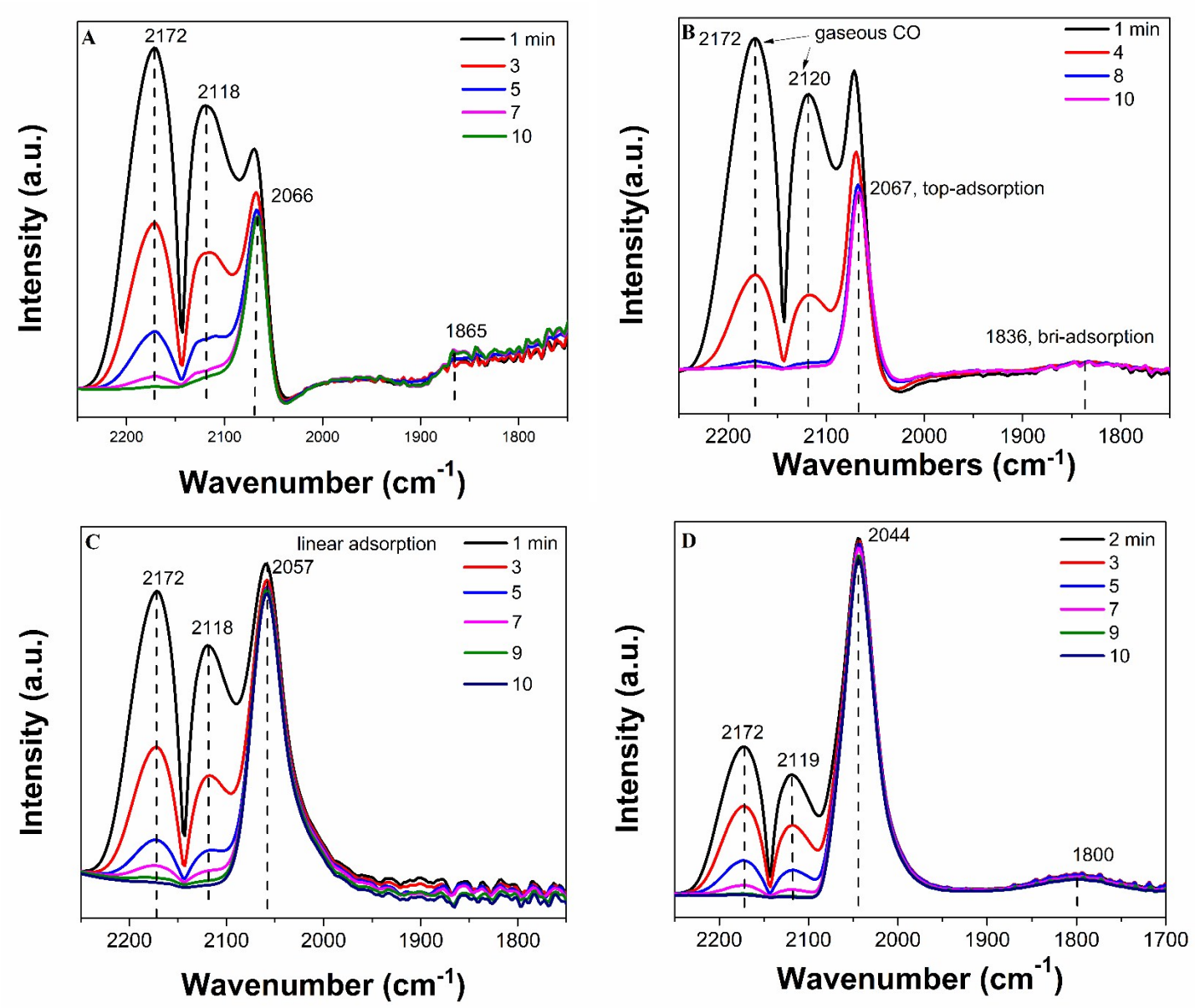

Figure S4. CO FTIR analysis of BiPt Bimetallic catalyst; CO adsorption before H_2 reduction: (A) 0.8Bi1Pt/ZSM-5, (B) 1Bi2Pt/SiO_2; CO adsorption after H_2 reduction: (C) 0.8Bi1Pt/ZSM-5, (D) 1Bi2Pt/SiO_2

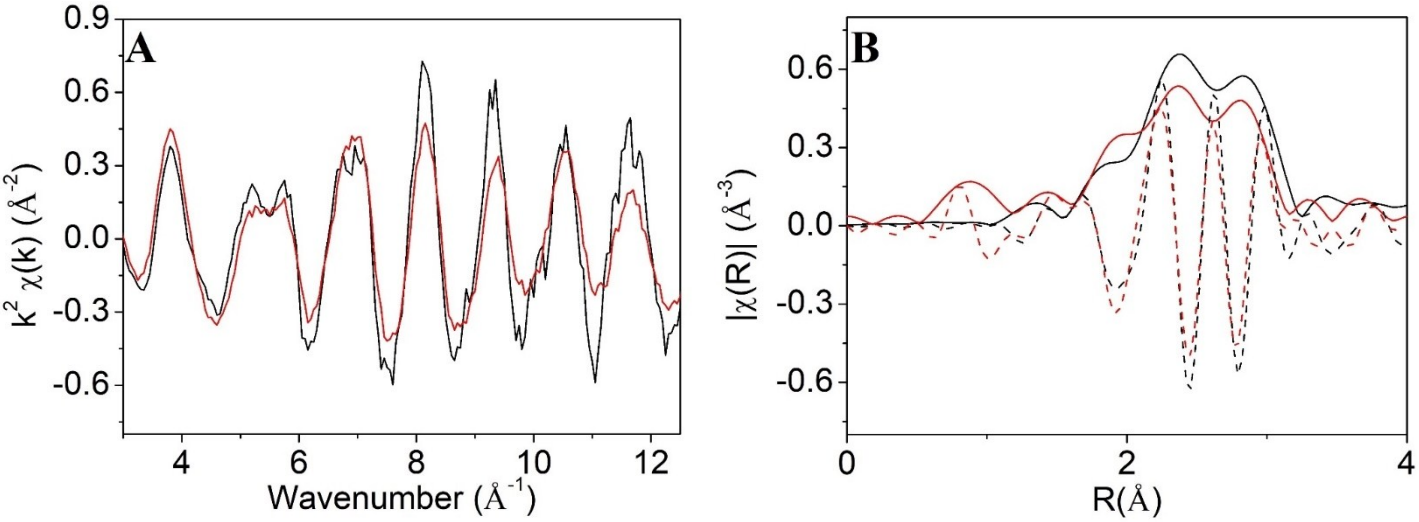

Figure S5. EXAFS comparison between 2Bi-2Pt/SiO_2 and 0.8Bi-1Pt/ZSM-5 (A) k^2-weighted χ (k) for 2Bi-2Pt/SiO_2 (black) and 0.8Bi-1Pt/ZSM-5 (red) (B) k^2-weighted Fourier transformation magnitude (dashed lines) and imaginary part (solid lines) of the EXAFS spectra for 2Bi-2Pt/SiO_2 (black) and 0.8Bi-1Pt/ZSM-5 (red)

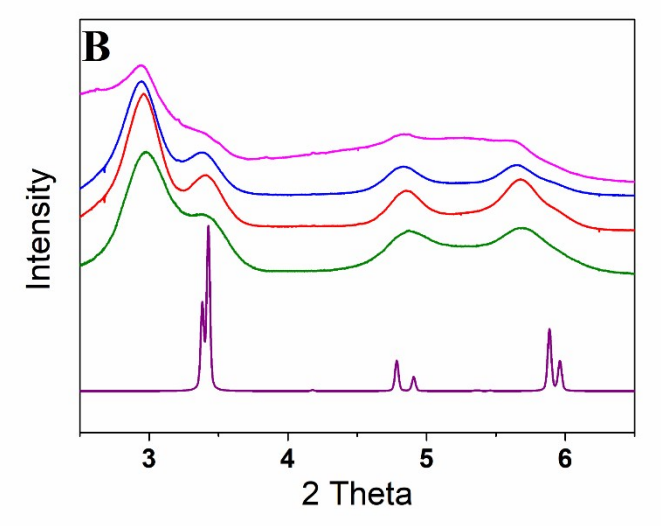

Figure S6. Simulated XRD patterns (A) XRD patterns of Pt-Bi bulk alloys and experimental Pt-Bi/SiO_2 taken at 550 °C (X-ray energy=105.715 keV). Pt_1Bi_1 simulation (black, ICSD:9008911), Pt_1Bi_2 simulation (navy, ICSD:9012345) (B) XRD patterns of simulated tetragonal Pt_1Bi_1 (AuCu structure type) and experimental Pt-Bi/SiO_2 taken at 550 °C (X-ray energy=105.715 keV). Tetragonal Pt_1Bi_1 simulation (purple, Pt-Pt bond distance=2.74 Å, Pt-Bi bond distance= 2.81 Å), Pt/SiO_2 (olive), 1Bi-2Pt/SiO_2 (red), 2Bi-2Pt/SiO_2 (blue), 4Bi-2Pt/SiO_2 (magneta).

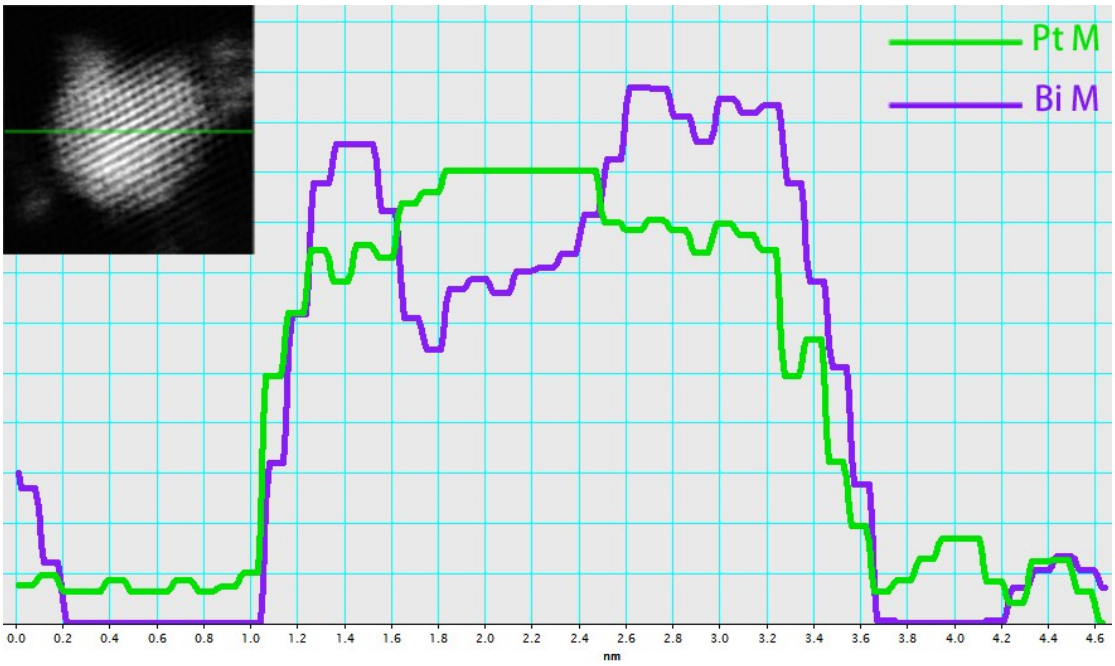

Figure S7. The extracted profile of Pt M and Bi M concentration across single PtBi bimetallic nanoparticle as show inset.

Table S1. XANES edge energy for the catalysts

Sample Name	XANES edge energy (keV)
$2Pt/SiO_2$	11.5640
$1Bi\text{-}2Pt/SiO_2$	11.5646
$2Bi\text{-}2Pt/SiO_2$	11.5647
$4Bi\text{-}2Pt/SiO_2$	11.5648
1Pt/ZSM-5	11.5640
0.1Bi-1Pt/ZSM-5	11.5641
0.8Bi-1Pt/ZSM-5	11.5646
1Bi-1Pt/ZSM-5	11.5646

Table S2. Peaks of the XRD spectra taken at 550°C

Sample Name	(111) peak (°)	(200) peak (°)	(220) peak (°)	(311) peak (°)
$2Pt/SiO_2$	2.980	3.430	4.881	5.712
$1Bi\text{-}2Pt/SiO_2$	2.959	3.404	4.861	5.680
$2Bi\text{-}2Pt/SiO_2$	2.942	3.378	4.835	5.650
$4Bi\text{-}2Pt/SiO_2$	2.937	-	-	-